MAPPING DEFORMATION OF MAN-MADE LINEAR FEATURES USING DINSAR TECHNIQUE

H. Wu [a, *], Y. Zhang [a], J. Zhang [a], X. Chen [b]

[a] Key Laboratory of Mapping from Space of State Bureau of Surveying and Mapping, Chinese Academy of Surveying and Mapping, Beijing 100830, China – wha_105@yahoo.com.cn, (yhzhang, zhangjx)@casm.ac.cn
[b] East China Institute of Technology, Nanchang 330013, China - chenxy@ecit.edu.cn

KEY WORDS: Monitoring, SAR, Technology, Image, Radar

ABSTRACT:

Man-made linear features like dams, highways, airports, and so on are very important infrastructures in any society. However, due to natural and human activities, ground deformation is threatening many linear features all over the world. Because of groundwater over-exploration, land subsidence has taken place in Taiyuan, China for many years. The South Ring Expressway and Wushu International Airport in the southern suburb of Taiyuan, is being threaten by severe ground subsidence. In this paper, 13 Envisat Advanced Synthetic Aperture Radar (ASAR) images from 2006 to 2009 have been acquired to monitor the southern Taiyuan City using small baseline differential interferometric SAR (DInSAR) technique. Along the South Ring Expressway, the maximum deformation lies in the central section, with an average velocity about -50 ~ -90 mm/a. The eastern section has the minimum deformation about -15 mm/a while the western section has a velocity about -10 ~ -50 mm/a. Over the Wushu International Airport, the deformation velocity is around -42 mm/a in the southwest and -20 mm/a in the northeast. Precise levelling data in the study area validate our results.

1. INTRODUCTION

Man-made linear features include dams, highways, railways, airports, oil or gas pipelines, and others. Most of them are vital infrastructures and facilities to sustain normal operation of any society. However, affected by natural and human activities, deformation is threatening many linear features all over the world. The deformation not only weakens the function of these man-made features, but also threatens the human life. Therefore, it is necessary to monitor the deformation timely and accurately and take corresponding measures to control it. Traditional ways of monitoring ground deformation utilize levelling and global positioning system (GPS) measurement. They have the advantage of high accuracy. However, they are very costly and can not achieve enough spatial sampling density.

With the development of radar remote sensing technique, differential interferometric SAR (DInSAR) is playing an important role in monitoring ground deformation. However, for long term deformation, conventional 2-pass or 3-pass DInSAR can be easily affected by temporal or geometric de-correlation which degrades the interferometric phase and makes it difficult to extract useful information (Ferretti, 1999). To solve this problem, some advances in this field have been introduced based on point target analysis, including permanent scatterers (PS) method (Ferretti, 2000, 2001; Vilardo, 2009), small baseline subsets (SBAS) method (Berardino, 2002, 2003a, 2003b, 2004; Casu, 2008) and coherent points (CP) method (Mora, 2003).

In this paper, the deformation in Taiyuan is investigated with time-series DInSAR analysis. Taiyuan, the capital of Shanxi Province, China, has been a city suffering water shortage severely. Over exploring groundwater has taken place in this city over 50 years, resulting in 4 significant subsidence centres in the urban area, namely Xizhang, Xiayuan, Wanbolin and Wujiapu (Sun, 2007). In recent years, with fast development of economy in the southern suburb, particularly the exploitation of Taiyuan Economic and Technological Development Zone, new subsidence centre has been found in this area, where the South Ring Expressway and Wushu International Airport are located. Therefore, it is urgent to monitor the deformation of this area. In this research, deformation maps around the South Ring Expressway and Wushu International Airport in Taiyuan are generated for the first time with small baseline DInSAR technique by combining PS and CP methods.

2. STUDY AREA AND DATASETS

2.1 Study area

The study area, Taiyuan, is located in the middle reaches of the Yellow River in North China. The Fenhe River, a key tributary of the Yellow River, runs through the territory of Taiyuan City over a distance of about 100 km. Taiyuan lies in a basin bounded by the Taihang Mountain Ranges in east and the Lvliang Mountain Ranges in west. The annual average precipitation in Taiyuan is 479 mm. Taiyuan is one of the cities lacking of water resources in China. The annual average capacity of water resource is 5.7×10^8 m^3 in this city. And the annual amount of water resources per capita is 172 m^3, which accounts for 46% of that in the whole province, or 6.6% of that in China. This is also the reason of over-exploring ground water in Taiyuan for a long time.

* Corresponding author.

2.2 Datasets

13 ENVISAT advanced synthetic aperture radar (ASAR) single look complex (SLC) images over the study area are acquired from February 2006 to February 2009. The temporal baselines and normal baselines are shown in Table 2. To remove the topographic phase from interferograms, digital elevation model (DEM) generated by Shuttle Radar Topography Mission (SRTM) with 3 arc-second resolution (about 90m) is used. In addition, 3 precise levelling measurements (Figure 1(b)) are utilized to validate the DInSAR experimental results.

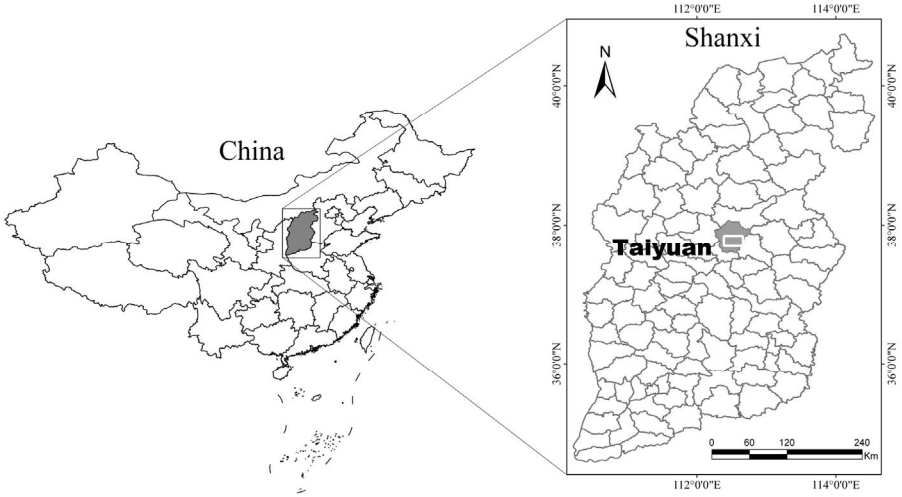

(a)

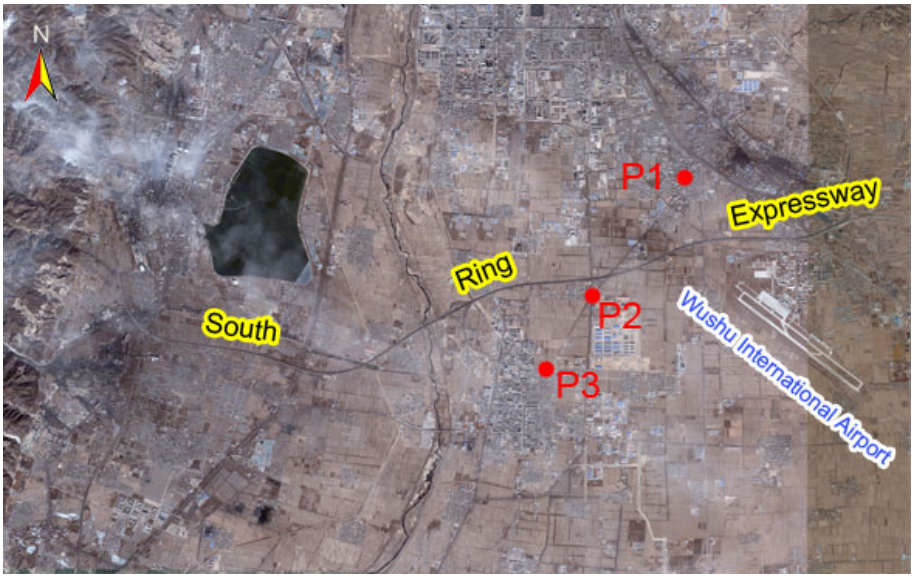

(b)

Figure 1. Study area: (a) location, (b) optical image provided by Google Earth with levelling points (red)

3. METHOD

There are two parts contained in the small baseline DInSAR technique, including linear deformation retrieval and non-linear deformation retrieval. Let us start our analysis by considering N SAR images acquired at the ordered times $(t_1,\cdots,t_N)$. We assume that each acquisition may interfere with at least another image and the normal baselines are small enough (e.g., 400m is chosen in this study) to reduce geometrical de-correlation. Based on N SAR images, we can generate M interferograms.

After removing the flat phase and topographic phase, each differential phase can be obtained, which can be expressed as

$$\phi_{dif\_i} = \phi_{def\_i} + \phi_{errortopo\_i} + \phi_{atm\_i} + \phi_{noise\_i} \quad (1)$$

where i is the i th interferogram, ϕ_{def} is the component due to the displacement of the terrain in satellite's look direction

between two SAR acquisitions, including linear deformation and non-linear deformation; $\phi_{errortopo}$ is the phase component

#	Date	Temporal Baseline /day	Normal baseline /m
1	2006-2-12	0	0
2	2006-11-19	280	-175
3	2007-1-28	350	-55
4	2007-3-4	385	759
5	2007-5-13	455	275
6	2007-9-30	595	223
7	2007-11-4	630	643
8	2007-12-9	665	-52
9	2008-1-13	700	403
10	2008-2-17	735	-2
11	2008-8-10	910	675
12	2008-12-28	1050	395
13	2009-2-1	1085	128

Table 2. ASAR images used in this research

due to the height error; ϕ_{atm} is the phase related with atmospheric artefacts; ϕ_{noise} is the noise phase including thermal noise, temporal and spatial decorrelation. The terms ϕ_{def} and $\phi_{errortopo}$ can be written as follows:

$$\phi_{errortopo} = \frac{4\pi}{\lambda} \cdot \frac{b}{r \cdot \sin\theta} \cdot \varepsilon \tag{2}$$

$$\phi_{def} = \frac{4\pi}{\lambda} \Delta r = \frac{4\pi}{\lambda} \cdot T \cdot v + \phi_{non-linear} \tag{3}$$

where λ is the wavelength; r the range distance; b the normal baseline; θ the incidence angle; ε and v are the height error and linear velocity; T is the temporal baseline between both SAR acquisitions.

Before linear deformation retrieval, high coherence point targets are selected according to pixel's coherence stability by setting a suitable coherence threshold for the mean coherence image. Based on these point targets, differential phase are connected with Delaunay triangulation. Thus the phase slope between two neighbouring points $(x_m, y_m), (x_n, y_n)$ on an edge can be expressed as

$$\begin{aligned}\delta\phi_{dif}(x_m, y_m, x_n, y_n, T_i) = {} & \frac{4\pi}{\lambda} \cdot T_i \cdot [v(x_m, y_m) - v(x_n, y_n)] \\ & + \frac{4\pi}{\lambda} \cdot \frac{b(T_i)}{r(T_i)\sin(\theta_i)} \cdot [\varepsilon(x_m, y_m) - \varepsilon(x_n, y_n)] \\ & + [\beta(x_m, y_m) - \beta(x_n, y_n)] \\ & + [\alpha(x_m, y_m) - \alpha(x_n, y_n)] \\ & + [n(x_m, y_m) - n(x_n, y_n)]\end{aligned} \tag{4}$$

where (x_m, y_m) and (x_n, y_n) are pixel position coordinates; T_i is the time baseline of the ith interferogram; β the nonlinear component of velocity; α the atmospheric phase artefacts; and n the decorrelation noise.

It is assumed that, within the atmospheric correlation range 1-3km, the atmospheric phases are equal, thus the atmospheric components can be neglected. For the linear deformation velocity and height error are constants, thus the above phase slope can be modelled as

$$\begin{aligned}\delta\phi_{model}(x_m, y_m, x_n, y_n, T_i) = {} & \frac{4\pi}{\lambda} \cdot T_i \cdot [\Delta v_{model}(m,n)] \\ & + \frac{4\pi}{\lambda} \cdot \frac{b(T_i)}{r(T_i)\sin(\theta_i)} \cdot [\Delta\varepsilon_{model}(m,n)]\end{aligned} \tag{5}$$

where Δv are $\Delta\varepsilon$ velocity and height error increments, respectively. They can be retrieved by maximizing the following Ensemble Phase Coherence (EPC) (Ferretti, 2000)

$$\gamma_{model}(x_m, y_m, x_n, y_n) = \frac{1}{M} \cdot \left| \sum_{i=0}^{M} \exp\begin{bmatrix} j \cdot (\delta\phi_{dif}(x_m, y_m, x_n, y_n, T_i) \\ -\delta\phi_{model}(x_m, y_m, x_n, y_n, T_i)) \end{bmatrix} \right| \tag{6}$$

where j is the imaginary unit, M is the number of interferograms. When the maximum EPC is close to 1, the velocity and height error increments are close to the real value. Then, the linear velocity and height error on each point target is obtained by integrating Δv_{model} and $\Delta\varepsilon_{model}$ with EPC over 0.7 from a starting reference point.

To retrieve non-linear deformation, it is necessary to calculate the model phase contributed by linear deformation and height errors. By subtracting the model phase from differential phase, we get residual phases, which mainly include atmospheric phase, non-linear deformation component and phase noises. Phase noises can be reduced by spatial low pass filtering. Atmospheric phase and non-linear deformation can be separated according to their different frequency characteristics in temporal and spatial domains (Ferretti, 2000; Mora, 2003).

4. RESULTS

4.1 Results

50 Interferograms with baselines of less than 400m are generated. 3335 high coherent point targets are selected from the average coherence. Using small baseline DInSAR technique described above, average deformation velocity and accumulated deformation over point targets are generated. Deformation around the South Ring Expressway and the Wushu International Airport from 2006 to 2009 are analyzed. Figure 3 shows the average subsidence velocity on sparse points and Figure 4 shows the whole subsidence field by spatial interpolation.

It can be found that, along the South Ring Expressway, 3 sections with different subsidence rates can be separated from each other. The west section from A to B deforms with a velocity of 10 ~ -50 mm/a The middle one from B to C has the largest velocity ranging from -50 to -90 mm/a while the east section from C to D has the smallest velocity of around -15 mm/a. The middle section of the expressway is close to the Taiyuan Economic and Technological Development Zone in Xiaodian District where a large amount of factories are located. Over-exploration of ground water has led to the largest subsidence in this area. The west and east sections contain mainly rural areas where ground water demands are less, so the subsidence rates are much less.

As far as the Wushu International Airport is concerned, deformation rates are also spatially varied. The average deformation velocity in the southwest reaches to about -42 mm/a, while in the northeast it is -20 mm/a.

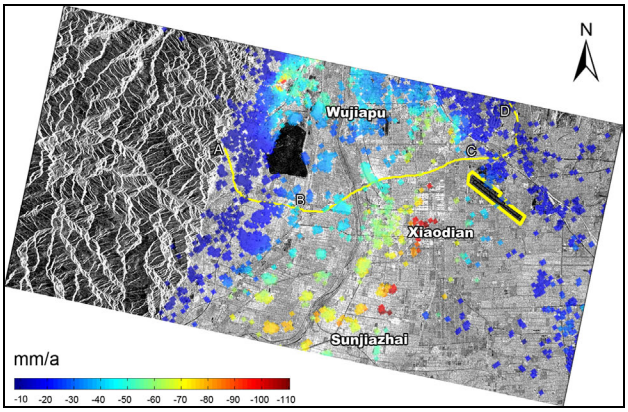

Figure 3. Average subsidence velocity in southern Taiyuan (2006-2009)

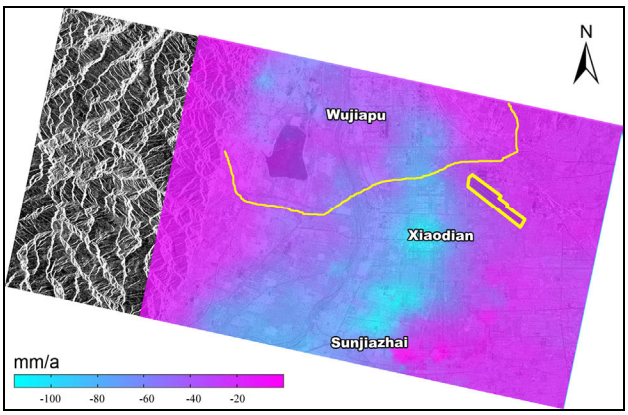

Figure 4. Subsidence field around expressway and airport (2006-2009)

4.2 Validation

To validate the DInSAR results, 3 levelling measurements, P1, P2 and P3 in the study area (Figure 1(b)), are used. Table 5 shows the comparison of the average deformation velocity between DInSAR results and levelling measurement. For the initial P3 measurement began in the end of 2006, the average deformation velocity at this point is not validated. From this table, it can be seen that the accuracy of DInSAR results at P1 and P2 is around -1.2 ~1.4 mm/a, demonstrating small baseline DInSAR technique can monitor ground deformation effectively. Besides the validation for average deformation velocity, we also compare the accumulative deformation on these 3 levelling points (Figure 6). The agreement between DInSAR results and levelling measurement is good.

Leveling points	DInSAR measurement	Leveling measurement	Errors
P1	-62.48	-61.33	-1.15
P2	-67.29	-68.67	1.38
P3	-63.25	-	-

Table 5. Comparison of average deformation velocity between DInSAR and levelling measurement (mm/a)

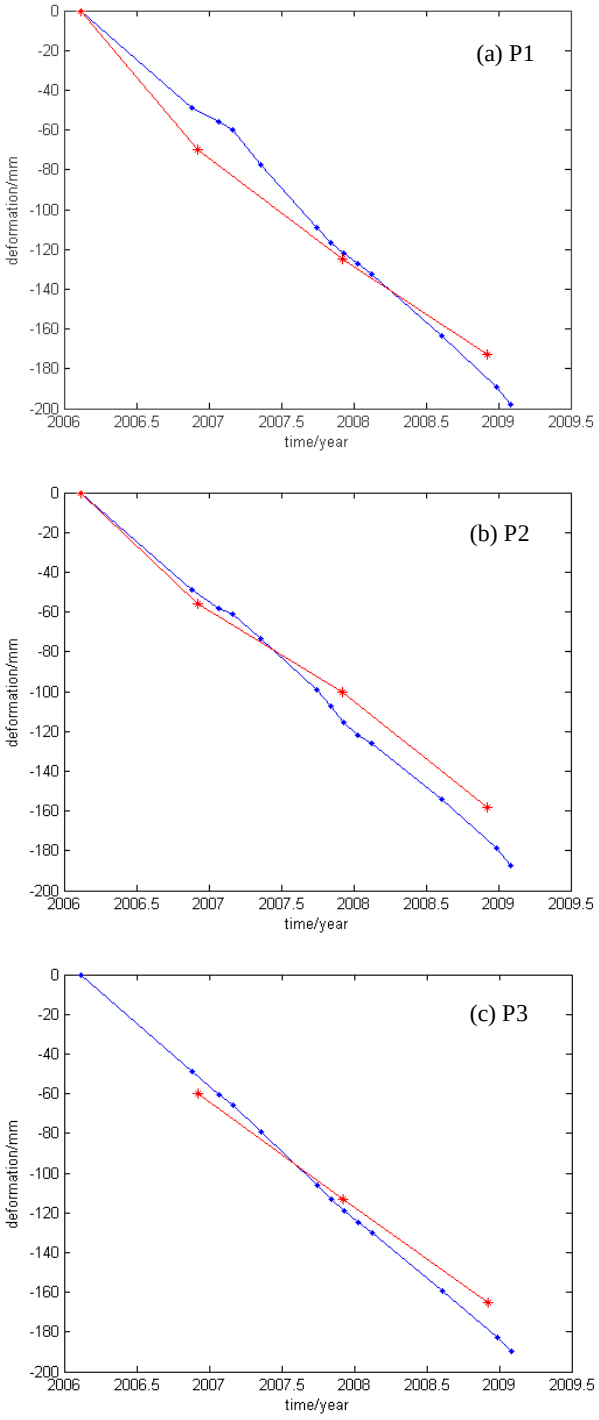

Figure 6. Comparison of accumulated deformation between DInSAR results (blue) and levelling measurements (red)

5. CONCLUSION AND DISCUSSION

Small baseline DInSAR technique combining the advantages of PS and CP methods has a great potential in deformation monitoring. Several characteristics of the technique can be summarized as the following: 1) it doesn't need as many SAR images as PS method; 2) it allows the generation of many small-

baseline multi-reference images to improve coherence; 3) it can derive linear and non-linear deformation fields at high coherence point targets.

We applied the technique to investigate ground deformation around the South Ring Expressway and Wushu International Airport in southern Taiyuan City. Along the South Ring Expressway, the maximum subsidence lies in the central section. The east section has the minimum subsidence and the west section has a medium subsidence velocity. Over the Wushu International Airport, the subsidence velocity is around -42 mm/a in the southwest and -20 mm/a in the northeast. The results suggest that the exploitation of Taiyuan Economic and Technological Development Zone in Xiaodian District has significant influence on local ground subsidence. Thus it is urgent to reduce ground water exploration in this area to control the subsidence.

REFERENCES

Berardino, P., Fornaro, G., Lanari, R., et al, 2002. A new algorithm for surface deformation monitoring based on small baseline differential SAR interferograms. *IEEE Trans Geosci Remote Sens*, 40(11), pp. 2375-2383.

Berardino, P., Casu, F., Fornaro, G., et al, 2003a. Small baseline DIFSAR techniques for earth surface deformation analysis. *FRING 2003 workshop*, Franscati, Italy.

Berardino, P., Fornaro, G., Lanari, R., et al, 2003b. A two-scale differential SAR interferometry approach for investigating earth surface deformations. *IGARSS 2003*, pp. 1184-1186.

Berardino, P., Casu, F., Lanari, R., et al, 2004. On the exploitation of the SBAS algorithm for the analysis of the deformations detected from the ERS and ENVISAT DInSAR data. *ERS-ENVISAT DInSAR Symposium*, 6–10 September 2004, Salzburg, Austria.

Casu. F., Manzo, M., Pepe, A., et al, 2008. SBAS-DInSAR Analysis of Very Extended Areas: First Results on a 60 000-km2 Test Site. *IEEE Trans. Geosci. Remote Sensing Letters*, 5 (3), pp. 438-442.

Ferretti, A., Rocca, F., Prati, C., 1999. Permanent scatterers in SAR interferometry. *IGARSS 1999*, Vol.3, pp.1528-1530

Ferretti, A., Prati, C., Rocca, F., 2000. Nonlinear subsidence rate estimation using permeanent scatterers in differential SAR interferometry. *IEEE Trans Geosci Remote Sens*, 28(5), pp. 2202-2212.

Ferretti, A., Prati, C., Rocca, F., 2001. Permanent scatterers in SAR interferometry. *IEEE Trans Geosci Remote Sens*, 39(1), pp. 8-20.

Mora, O., Mallorqui, J., Broquetas, A., 2003. Linear and nonlinear terrain deformation maps from a reduced set of interferometric SAR images, *IEEE Trans Geosci Remote Sens*, 41(10), pp. 2243-2253.

Sun, Z., Ma, T., Ma, J., et al, 2007. Effect of strata heterogeneity on spatial pattern of land subsidence in Taiyuan City. *Rock and Soil Mechanics*, 28 (2), pp. 399-408.

Vilardo, G., Ventura. G., Terranova. C., et al, 2009. Ground deformation due to tectonic, hydrothermal, gravity, hydrogeological, and anthropic processes in the Campania Region (Southern Italy) from Permanent Scatterers Synthetic Aperture Radar Interferometry. *Remote Sensing of Environment*, 113, pp. 197-212.

ACKNOWLEDGEMENTS

This research is supported by the National Key Basic Research and Development Program, China, under project number 2006CB701303, and Taiyuan Water Resources Bureau under the project, “Ground Subsidence Monitoring in Taiyuan Using Spaceborne InSAR Technique”. ENVISAT ASAR data are copyrighted and provided by European Space Agency (ESA). The authors would like to thank Dr. Zhong Lu (USGS) for his suggestive discussion and careful review. They also thank the Taiyuan Water Resources Bureau for the levelling data which validate DInSAR results in this research.